2024 20th IEEE/ASME International Conference on Mechatronic and Embedded Systems and Applications (MESA) | 979-8-3315-1623-9/24/$31.00 ©2024 IEEE | DOI: 10.1109/MESA61532.2024.10704823

Task Space Trajectory Planning for an Articulated Dielectric Elastomer Soft Robot with Input Saturation and Underactuation

Giovanni Soleti
Department of Systems Engineering
Saarland University
Saarbruecken, Germany
giovanni.soleti@imsl.uni-saarland.de

Lorenzo Cicali
Department of Electrical and Automation Engineering
University of Florence
Florence, Italy
lorenzo.cicali1@edu.unifi.it

Michael Franci
Department of Electrical and Automation Engineering
University of Florence
Florence, Italy
michael.franci@unifi.it

Luca Pugi
Department of Electrical and Automation Engineering
University of Florence
Florence, Italy
luca.pugi@unifi.it

Gianluca Rizzello
Department of Systems Engineering
Saarland University
Saarbruecken, Germany
gianluca.rizzello@imsl.uni-saarland.de

***Abstract*—In this paper we propose a new trajectory planning algorithm for an underactuated soft robot based on dielectric elastomer actuators. The planning of the dynamic trajectories is addressed by accounting for the constraints imposed by the underactuated nature of the robot, the physical limits of its operational space, as well as control input saturation. After deriving all the feasible equilibrium configurations of the robot, a trajectory planning algorithm is proposed to achieve a desirable motion in the configuration space of the system. The obtained trajectories provide a feasible reference for trajectory tracking motion control algorithms. The effectiveness of the approach is verified via numerical simulations conducted on an experimentally validated, physics-based model of the system.**

***Index Terms*—Trajectory planning, task-space control, tracking control, underactuated robot, soft-robotics, dielectric elastomer.**

I. Introduction

Soft robotic systems mark a significant stride in bridging the gap between biological organisms and conventional rigid robots [1]. Soft robotic design principles embrace elasticity and flexibility, which are crucial for adaptability and versatility. The integration of soft attributes such as flexibility and compliance into robotic frameworks presents unique challenges in control, design, and modeling [2]. The complexity of models increases notably considering the high (theoretically infinite) number of degrees of freedom, often resulting in underactuation and presence of material elastic nonlinearities.

While most of the soft robots presented in literature focus on tendon-driven or pneumatic systems [3], [4], this paper considers an articulated soft robotic system driven by dielectric elastomer (DE) transducers [5]. DEs are smart materials able to change their shape when subjected to high voltage. DE actuators (DEAs) are energy efficient, highly stretchable, and soft, thus they are particularly attractive for soft robotics applications. DEAs also feature self-sensing capabilities, enabling cost-effective implementation of closed-loop controllers without using expensive sensors like cameras or laser transducers [6]. The DE soft robot considered in this work is depicted in Fig. 1a. It exhibits a T-shaped structure made of two rigid plates connected by a soft flexible backbone, which is compressed by two pre-tensioned rolled DEAs. The stiffness of the DEAs is reduced when a high voltage is applied to their electrodes, causing bending to the right-hand and left-hand side respectively, depending on which actuator is activated, cf Fig. 1c and Fig.1d. By design the system to be open-loop bistable, the system can achieve a large actuation displacement (up to ±25°) compared to a monostable design (±5°), see [7] for details. Despite bringing this advantage, the bistable design makes it no longer possible to control the motion of the robot in a proportional way. Although in principle this issue can be solved via feedback control, its practical achievement it is highly challenging due to the underactuated nature of the robot as well as the presence of actuation and input saturation nonlinearities.

While different work has been proposed to achieve a motion control of single degree-of-freedom DEAs [8] [9] [10], for more complex system the literature is restricted to few works. In a recent work [11], the authors proposed a method that takes ispiration from the joint-space trajectory tracking of rigid robots. The developed control law guarantees that a predefined

The authors gratefully acknowledge the support of the Deutsche Forschungsgemeinschaft (DFG, German Research Foundation through Priority Program SPP 2100 “Soft Material Robotic Systems” (Projects: SE704/6-2, RI3030/1-2).

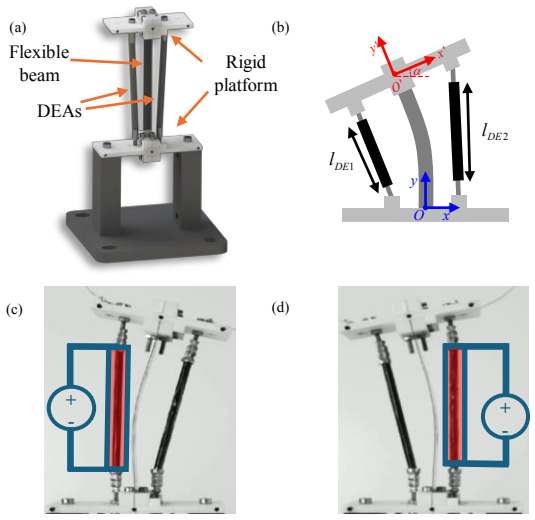

Fig. 1. Considered system and actuation principle: (a) single module; (b) design of the prototype; (c) left DEA actuated; (d) right DEA actuated.

trajectory is tracked on the actuation coordinates for the above described soft robot, which are represented by the length of the DEAs. In real applications, however, the trajectory is expected to be planned in terms of task space coordinates rather than the actuation ones. While planning trajectories in actuation spaces is straightforward, the corresponding planning problem in task space is made especially challenging by the underactuated and strongly nonlinear nature of the system. In this paper, the proposed tracking controller is used for the first time to achieve a desired motion control in the DEA soft robot task space. While trajectory planning is already solved for rigid and flexible robots [12], [13], the problem is still largely unexplored in the field of soft robotics. The proposed algorithm is designed for a system which has several features in common with other soft-robots, and that poses challenges to the trajectory planning task, such as underactuation, configuration dependent actuation matrix (CDAM), control input saturation, and strong elastic nonlinearities. As first step, the robot static workspace is characterized by finding all the feasible equilibria of the system with a numerical algorithm. Based on this, an algorithm to plan trajectories in the task-space without violating input saturation is proposed. The effectiveness of the approach in generating feasible trajectories is verified via numerical simulations.

The remainder of this paper is organized as follows. In Section II, we present the system model. Section III discusses the evaluation of all the possible feasible equilibrium points and propose the trajectory planning algorithm, while Section IV demonstrates the effectiveness of the results through numerical simulations. Finally, concluding remarks are discussed in Section V.

II. Modeling and Trajectory Tracking Control

A physics-based model of the system is first presented in this section, for which a trajectory tracking control law is subsequently proposed based on our previous results in [11].

A. Generalized coordinate system-modeling

For the sake of conciseness, only the necessary details about the model are provided in this section, for more details the reader may refer to [11]. The dynamic response of the DE soft robot shown in Fig. 1b is described by

$$M\ddot{q} + D(q)\dot{q} + G(q) = J^{\intercal}(q), \tag{1}$$

where $q = \begin{bmatrix} q_x & q_y & \alpha \end{bmatrix}^{\intercal} \in \mathbb{R}^3$ are the generalized coordinates, chosen as the coordinates, and the angular displacement of the rigid plate in the body frame $O'(x', y')$ relative to the static reference frame $O(x, y)$. Matrices $M \succ 0$ and $D(q) \succ 0$ describe inertia and dissipation, while $G(q)$ contains forces due gravity, DEAs hyperelasticity, and the flexible backbone. Open-loop bistability implies that

$$\frac{\partial G(q)}{\partial q} \not\succ 0,$$

for some $q \in \mathbb{R}^3$. The actuation matrix $J(q) \in \mathbb{R}^{2\times 3}$ is obtained by

$$J(q) = \frac{\partial l_{DE}(q)}{\partial q},$$

where $l_{DE}(q) = \begin{bmatrix} l_{DE1}(q) & l_{DE2}(q) \end{bmatrix}^{\intercal} \in \mathbb{R}^2$ represents the actuators lengths in function of the generalized coordinate, illustrated on Fig. 1b.

Finally, $u \in \mathbb{R}^2$ represents the control input of the system and is defined by $u = \begin{bmatrix} u_1 & u_2 \end{bmatrix}^{\intercal} = \begin{bmatrix} \beta v_{DE1}^2 & \beta v_{DE2}^2 \end{bmatrix}^{\intercal}$, where v_{DEi} is the voltage applied to DEA i, $i = 1, 2$, and β is a parameter that models the geometry of the DEAs actuator. Note that, for the actuators considered in this work

$$0 \leq v_{DEi} \leq \hat{v}_{DE}, \quad i = 1, 2,$$

with $\hat{v}_{DE} = 3000$ V maximum voltage applicable to the actuators. Thus, by introducing the set of the feasible input $\mathcal{U} = \begin{bmatrix} 0, & \hat{u} \end{bmatrix} \times \begin{bmatrix} 0, & \hat{u} \end{bmatrix} \subset \mathbb{R}^2$, with $\hat{u} = \beta \hat{v}_{DE}^2$, any feasible control input must satisfy $u(t) \in \mathcal{U}\ \forall t$.

The presented model is validated experimentally, as shown in Fig. 2. The identification procedure is carried out by using standard nonlinear optimization tool in the MATLAB environment. In Fig. 2 is shown how the model match the experiments with a FIT of 89.7%.

B. Control-oriented change of coordinates

The system in (1) has CDAM and is underactuated with 3 degrees of freedom and 2 actuators, which makes it challenging to control. In recent work [14] it is shown that, under certain conditions, a change of coordinate which brings an underactuated Lagrangian system with CDAM to the so-called collocated form exist, in this form the inputs are decoupled thus simplifying the development of control strategies. Building on this result, in [11] we found a suitable change of

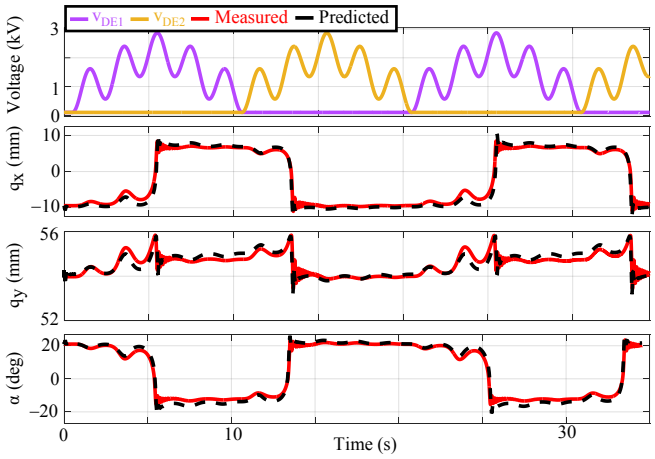

Fig. 2. Experimental identification of the presented system.

coordinates to bring the DE soft robot model in collocated form. The new set of coordinates z is

$$z\left(q\right) = \begin{bmatrix} z_a\left(q\right) \\ z_u\left(q\right) \end{bmatrix}$$

where, according to [14] $z_a\left(q\right) = l_{DE}\left(q\right) \in \mathbb{R}^2$ are the actuator coordinates, while $z_u\left(q\right) = \alpha \in \mathbb{R}$. This choice for the new coordinates permits to find an analytical inverse of the map from q and z within a well-defined subset of the configuration space $\mathcal{Q} \subset \mathbb{R}^3$. By omitting the dependencies by z of the system matrix for the ease of conciseness, the system equations in the new set of coordinates are

$$\begin{bmatrix} M_{z_{aa}} & M_{z_{au}} \\ M_{z_{ua}} & M_{z_{uu}} \end{bmatrix} \begin{bmatrix} \ddot{z}_a \\ \ddot{z}_u \end{bmatrix} + \begin{bmatrix} \zeta_a \\ \zeta_u \end{bmatrix} = \begin{bmatrix} u \\ 0 \end{bmatrix}, \tag{2}$$

where M_z is the mass-matrix in the new set coordinates, and

$$\zeta_a = \left(C_{z_{aa}} + D_{z_{aa}}\right)\dot{z}_a + \left(C_{z_{au}} + D_{z_{au}}\right)\dot{z}_u + G_{z_a},$$
$$\zeta_u = \left(C_{z_{ua}} + D_{z_{ua}}\right)\dot{z}_a + \left(C_{z_{uu}} + D_{z_{uu}}\right)\dot{z}_u + G_{z_u}.$$

Differently from (1), the system in the new set of coordinate (2), presents different advantages. In particular, model (2) recalls the structure of a flexible robot, for which the partial feedback linearization approach presented in [15] permits to develop a control law that ensures that z_a follows an arbitrary reference trajectory $z_a^\star$. In particular, as presented for the first time in [11], the control law

$$u = \zeta_a - M_{z_{au}} M_{z_{uu}}^{-1} \zeta_u + \tilde{M}_z \left(\ddot{z}_a^\star - K_D \dot{\tilde{z}}_a - K_P \tilde{z}_a\right) \tag{3}$$

with $\tilde{z}_a = z_a - z_a^\star$ and $\tilde{M}_z$ representing the the Schur's complement of the block $M_{z_{uu}}$ of the matrix M_z, stabilizes the tracking error

$$\lim_{t\to\infty} \left\| z_a\left(t\right) - z_a^\star\left(t\right) \right\| = 0.$$

III. Trajectory Planning Strategies

The control algorithm presented in Section II.B ensures that the closed loop system tracks a trajectory in the z_a coordinates, while practical tasks require trajectories to be planned in task space coordinates q. This section aims to provide an algorithm that practically solves the problem of generating a feasible trajectory z_a starting from a desired trajectory in q, which evolves from a given q_{start} to q_{end}, that are two equilibrium configurations of the system, with a desired trajectory in between. This problem is challenging for two main reasons, namely the fact that $z_a \in \mathbb{R}^2$ while $q \in \mathbb{R}^3$, and that not all trajectories result in u within their physical limits. To tackle those issues, we provide an algorithm that finds all the feasible equilibrium configurations, and based on this we generate feasible trajectories in the robot task space q.

A. Preliminaries Equilibrium Study

The search of the equilibrium is an important step because permits to understand which is the achievable motion range of the system. The analysis is conducted in the system in z coordinates. First, we obtain a mesh by gridding l_{DE1}, l_{DE2}, and α within feasible working ranges. By considering the choice of variables z, the following meaningful ranges for the gridding can be established via physical consideration

$$1.1 \leq \frac{l_{DEi}}{L_1} \leq 1.7, \quad i = 1, 2 \tag{4a}$$
$$-25^\circ \leq \alpha \leq 25^\circ, \tag{4b}$$

where L_1 is the unstretched length of the dielectric elastomers. The condition (4a) is directly related to the maximum elongation of the single RDEA actuator, while (4b) is obtained by considering the maximum range of motion of the structure. A general equilibrium of the system is obtained by imposing $\dot{z} = 0$, and $\ddot{z} = 0$ in the equations of motion (2). The equilibrium configuration $\bar{z}$ and the corresponding equilibrium input $\bar{u}$ are obtained by solving

$$\begin{bmatrix} G_a\left(\underline{z}\right) \\ G_u\left(\underline{z}\right) \end{bmatrix} = \begin{bmatrix} \underline{u} \\ 0 \end{bmatrix}. \tag{5}$$

Note that, given input $\underline{u}$, the solution of (5) is not necessarily unique. A suitable solution of (5) must also satisfies $\underline{z} \in \mathcal{Q}$ and $0 \leq \underline{u}_i \leq \hat{u}$, $i = 1, 2$. In particular, the belonging of $\underline{z}$ to $\mathcal{Q}$ depends only the kinematic parameters of the system, and is verified if the conditions proposed in the Proposition 3 of [11] are satisfied. Alternatively, before that the procedure starts, it is possible to build the set $\mathcal{Q}$ by gridding on the possible value of l_{DE1}, l_{DE2}, and α.

Due to the high nonlinearities of the system, the equilibrium equation (5) cannot be analytically solved. Based on the algorithm 1 proposed in Section III-A, a solution that tackles this problem is obtained by analyzing the critical points of the potential energy respect to α.

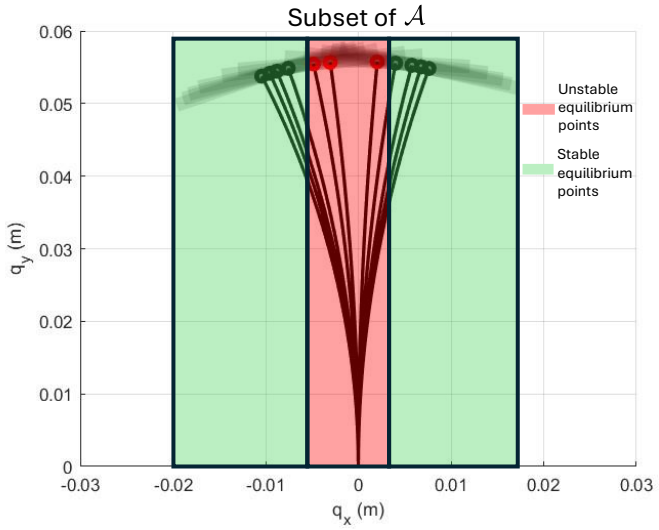

Fig. 3. Subset of the set $\mathcal{A}$.

Algorithm 1 Search of the equilibrium point

```
Initialize the kinematic and dynamic parameters in the system equations (1);
Perform the change of coordinate, and obtain the system equations (2);
Initialize A = ∅;
for each possible l_DE1 do
    for each possible l_DE2 do
        obtain the vector [l_DE1  l_DE2]^T;
        for each possible α do
            if z = [l_DE1  l_DE2]^T then
                calculate G_zu(z);
                if G_zu(z) = 0 then
                    calculate G_za(z);
                    if if G_za(z) ∈ U then
                        select z and obtain q by the coordinate transformation proposed in [11];
                        add q to A;
                    end if
                end if
            end if
        end for
    end for
end for
```

The outcome of the Algorithm 1, is shown in Fig. 3 where a subset of $\mathcal{A}$ is drawn. Due to the bistability of the system, the (locally) open-loop stable equilibrium points are distributed in the two regions on the left-hand and right-hand sides of the motion range of the system, while all the unstable equilibrium points are concentrated near the vertical configuration. Note that, the stability is evaluated in open-loop by calculating the eigenvalue of the local stiffness matrix in the equilibrium.

B. Trajectory Planning

The algorithm starts with a trajectory planning over variable α. A generic smooth trajectory can be assigned in this phase using as start and end point the corresponding third component of q_{start} and q_{end}, and making sure that both velocity and acceleration are zero at both initial and final times (this goal is achievable using a 5^{th} order polynomial trajectory). After that, the trajectory over q_y is obtained by an interpolation of the static workspace considering the corresponding values of α in $\mathcal{A}$. Due to high sensitivity of the system to the vertical displacement, a 10^{th} order interpolating polynomial is used. A correction term is injected to the planned trajectory of q_y based on a 9^{th} order polynomial, defined by choosing to zero initial and final position, velocity, and acceleration, and using the remaining four free parameters to design a small hump at a given location. The size and location of this hump are designed in order to correct small numerical errors arising from the beam near incompressibility ($\alpha = 0$), which would otherwise result in trajectories requiring excessively large control inputs nearby the vertical configuration. After that, the resulting trajectory over q_x is obtained by solving the zero-dynamics equation

$$J_0^{\intercal}(q)\left(M\ddot{q} + D(q)\dot{q} + G(q)\right) = 0, \tag{6}$$

where $J_0(q) \in \mathbb{R}^{3\times 1}$ is a full-rank right annihilator of $J(q)$. In particular, dynamic system (6) can be seen as a input-output system where $\ddot{\alpha}, \dot{\alpha}, \alpha$, and $\ddot{q}_y, \dot{q}_y, q_y$ are the input while $\ddot{q}_x, \dot{q}_x, q_x$ represent the outputs. After that a trajectory is generated, a feasibility analysis is performed by verifying that the input of the open-loop system along the trajectories, computed as

$$\bar{u} = M_{z_{aa}}(\bar{z})\,\ddot{\bar{z}}_a + M_{z_{au}}(\bar{z})\,\ddot{\bar{z}}_u + \zeta_a(\dot{\bar{z}}, \bar{z}),$$

is within the feasible saturation set $\mathcal{U}$. The procedure is summarized by Algorithm 2.

As a final remark, we point out that the choice of α, and q_y as input of the trajectory generation is purely arbitrary. In this work, we choose to plan the trajectory over α because it is the degree of freedom that characterize the general motion of the structure, while q_y represents the vertical compression of the beam and thus it is a less interesting quantity from the application standpoint.

IV. Simulation Results

In this section, the effectiveness of the planning strategy is validated with two different trajectories generated with the algorithms proposed in Section III. To achieve the motion tracking on the actuator coordinates, the control law (3) is applied with $K_p = 100I$, and $K_d = 10I$. In Fig. 4 we present a 5^{th} order polynomial trajectory that cover all the operational space. The trajectory is generated with the Algorithm 2 proposed in Section III. It is readily observed that the planned trajectory is satisfactorily tracked while the input is kept within the saturation limits of the actuators. The proposed planning method ensures smooth trajectories at each time,

Algorithm 2 Trajectory Generator Algorithm

Define a max number of iteration max_iter;
Set $iter$ = 0
Choose the duration of the trajectory;
Choose α_{start}, and α_{end}, and plan a smooth trajectory on α;
Calculate $\ddot{\alpha}$, and $\dot{\alpha}$;
Define a generic 10^{th} order trajectory that interpolates q_y in the set $\mathcal{A}$, and calculates the corresponding $\ddot{q}_y, \dot{q}_y$;
Main Loop
Calculate $\ddot{q}_x, \dot{q}_x, q_x$ from the zero dynamics equations (6);
Obtain the trajectory in coordinate z, and the corresponding input $\underline{u}(t)$ from (2);
while $(\exists \underline{u}(t) \notin \mathcal{U})$ **and** $iter \ \leq max\_iter$ **do**
    define a new hump peak and its instant of time;
    plan a 9^{th} order disturbance trajectories to sum on q_y;
    obtain the new $\ddot{q}_y, \dot{q}_y, q_y$;
    Repeat Step 7;
    Repeat Step 8 to obtain $\underline{u}(t)$;
    $iter$ = $iter$ + 1;
end while
if $iter \leq max\_iter$ **then**
    Return the valid trajectory;
else
    Repeat from Step 1;
end if

thus successfully eliminating oscillations in the closed loop configuration variables which are observed when planning the trajectories directly in actuator space, previously reported in [11]. In Fig. 5, instead, a different trajectory consisting in a sinusoidal wave trajectory on α is planned. In this case, it can be observed how the trajectory on q_x, and α is sinusoidal, while on q_y there is a peak in correspondence of $\alpha = 0$ due to the beam nonlinearities. Also here, limits on the control input saturation are satisfied.

V. Conclusion

In this paper, a task space trajectory planning algorithm for an underactuated DE soft robot is proposed for the first time. The problem is solved by taking in account different characteristics common to many soft robots, such as underactuation, CDAM, and control input saturation. For the given DE soft robot, an algorithm is proposed to generate a feasible task space trajectory which is compatible with its dynamics and does not violate saturation limit. The planned task space trajectory is then used to derive the corresponding actuator space trajectory, which in turn is used as a reference in a partial feedback linearization control algorithm. Based on numerical simulations, the effectiveness of the approach is established. Moreover, the method allows to eliminate unwanted oscillations which are instead observed when planning the trajectories in actuation space. While established and studied for the DE soft robots, the previous algorithm can in principle be applied to any soft robot that presents similar

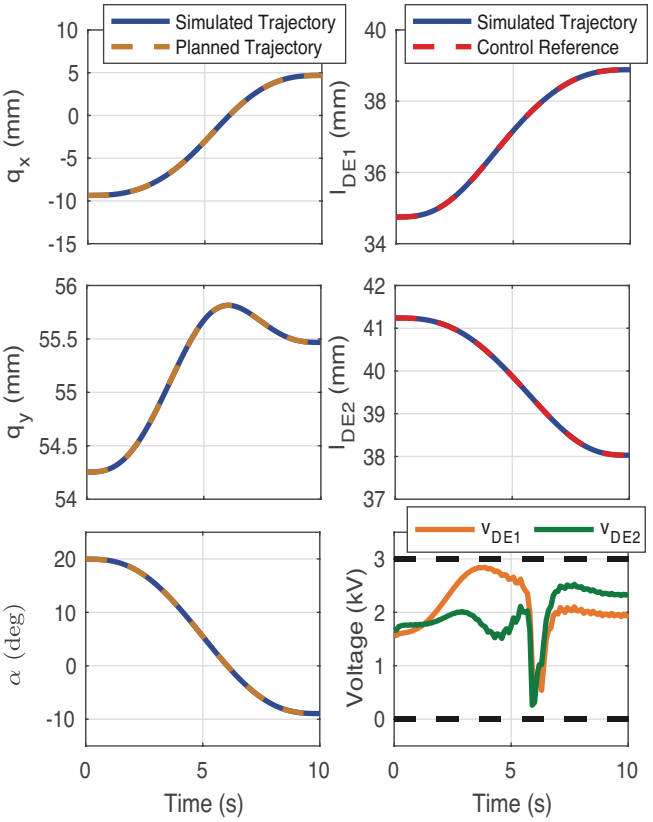

Fig. 4. 5th order polynomial planned trajectory on α.

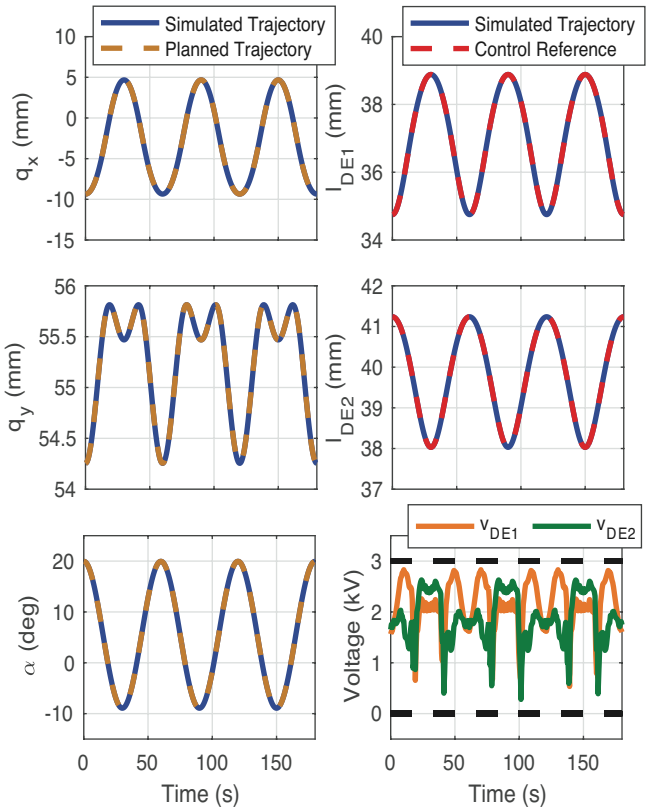

Fig. 5. Sinusoidal trajectory on α with a period of 60s.

characteristics, such as tendon-driven ones. Future works will focus on enhancing the robustness to parameters uncertainties, and by validating the control algorithm experimentally based on the planned trajectory.

REFERENCES

[1] S. Kim, C. Laschi, and B. Trimmer, "Soft robotics: a bioinspired evolution in robotics," *Trends in biotechnology*, vol. 31, no. 5, pp. 287–294, 2013.

[2] J. Wang and A. Chortos, "Control strategies for soft robot systems," *Adv. Intell. Syst.*, vol. 4, no. 5, Feb. 2022.

[3] M. S. Xavier, C. D. Tawk, A. Zolfagharian, J. Pinskier, D. Howard, T. Young, J. Lai, S. M. Harrison, Y. K. Yong, M. Bodaghi, *et al.*, "Soft pneumatic actuators: A review of design, fabrication, modeling, sensing, control and applications," *IEEE Access*, vol. 10, pp. 59 442–59 485, 2022.

[4] U. Jeong, K. Kim, S.-H. Kim, H. Choi, B. D. Youn, and K.-J. Cho, "Reliability analysis of a tendon-driven actuation for soft robots," *The International Journal of Robotics Research*, vol. 40, no. 1, pp. 494–511, 2021.

[5] P. Brochu and Q. Pei, "Advances in dielectric elastomers for actuators and artificial muscles," *Macromolecular Rapid Communications*, vol. 31, no. 1, pp. 10–36, 2010.

[6] K. Jung, K. J. Kim, and H. R. Choi, "A self-sensing dielectric elastomer actuator," *Sensors and Actuators A: Physical*, vol. 143, no. 2, pp. 343–351, 2008.

[7] M. Baltes, J. Kunze, J. Prechtl, S. Seelecke, and G. Rizzello, "A bi-stable soft robotic bendable module driven by silicone dielectric elastomer actuators: design, characterization, and parameter study," *Smart Mater. Struct.*, vol. 31, no. 11, p. 114002, 2022.

[8] P. R. Massenio, G. Rizzello, and D. Naso, "Fuzzy adaptive dynamic programming minimum energy control of dielectric elastomer actuators," in *2019 IEEE International Conference on Fuzzy Systems (FUZZ-IEEE)*. IEEE, 2019, pp. 1–6.

[9] F. Branz and A. Francesconi, "Modelling and control of double-cone dielectric elastomer actuator," *Smart Materials and Structures*, vol. 25, no. 9, p. 095040, 2016.

[10] P. R. Massenio, G. Rizzello, G. Comitangelo, D. Naso, and S. Seelecke, "Reinforcement learning-based minimum energy position control of dielectric elastomer actuators," *IEEE Transactions on Control Systems Technology*, vol. 29, no. 4, pp. 1674–1688, 2020.

[11] G. Soleti, P. R. Massenio, J. Kunze, and G. Rizzello, "Nonlinear coordinate transformation and trajectory tracking control of an under-actuated soft robot driven by dielectric elastomers," in *2024 IEEE 7th International Conference on Soft Robotics (RoboSoft)*, 2024, pp. 228–234.

[12] L. Sciavicco and B. Siciliano, *Modelling and control of robot manipulators*. Springer Science & Business Media, 2012.

[13] A. De Luca and W. J. Book, "Robots with flexible elements," *Springer handbook of robotics*, pp. 243–282, 2016.

[14] P. Pustina, C. Della Santina, F. Boyer, A. De Luca, and F. Renda, "Input decoupling of lagrangian systems via coordinate transformation: General characterization and its application to soft robotics," *IEEE Transactions on Robotics*, 2024.

[15] M. W. Spong, "Partial feedback linearization of underactuated mechanical systems," in *Proceedings of IEEE/RSJ International Conference on Intelligent Robots and Systems (IROS'94)*, vol. 1. IEEE, 1994, pp. 314–321.